HHS Public Access

Author manuscript

Cell Mol Gastroenterol Hepatol. Author manuscript; available in PMC 2016 December 15.

Published in final edited form as:

Cell Mol Gastroenterol Hepatol. 2016 May ; 2(3): 340–357. doi:10.1016/j.jcmgh.2016.01.006.

Critical role of PepT1 in promoting colitis-associated cancer and therapeutic benefits of the anti-inflammatory PepT1-mediated tripeptide KPV in a murine model

Emilie Viennois[1,2,*], **Sarah A. Ingersoll**[1,#], **Saravanan Ayyadurai**[1,#], **Yuan Zhao**[1,3], **Lixin Wang**[1,2], **Mingzhen Zhang**[1], **Moon Kwon Han**[1], **Pallavi Garg**[1], **Bo Xiao**[1], and **Didier Merlin**[1,2]

[1]Institute for Biomedical Sciences, Center Diagnostics and Therapeutics, Georgia State University, Atlanta, GA

[2]Veterans Affairs Medical Center, Decatur, GA

[3]Department of Gastroenterology, Zhongshan Hospital, Fudan University, China

Abstract

Background and aims—The human intestinal peptide transporter 1, hPepT1, is expressed in the small intestine at low levels in the healthy colon and upregulated during inflammatory bowel disease. hPepT1 plays a role in mouse colitis and human studies have demonstrated that chronic intestinal inflammation leads to colorectal cancer (colitis-associated cancer; CAC). Hence, we assessed here the role of PepT1 in CAC.

Methods—Mice with hPepT1 overexpression in intestinal epithelial cells (TG) or PepT1 (PepT1-KO) deletion were used and CAC was induced by AOM/DSS.

Results—TG mice had larger tumor sizes, increased tumor burdens, and increased intestinal inflammation compared to WT mice. Conversely, tumor number and size and intestinal inflammation were significantly decreased in PepT1-KO mice. Proliferating crypt cells were increased in TG mice and decreased in PepT1-KO mice. Analysis of human colonic biopsies

[*]Correspondence: Institute for Biomedical Sciences, Georgia State University, 100 Piedmont Avenue, PSC 757, Atlanta, GA, 30303, Tel: 404 413 3598; Fax: 404 413 3580, eviennois@gsu.edu.
[#]These authors equally contributed to this work

Disclosure: The authors have nothing to disclose.

Author contributions:
EV: Study concept and design, acquisition of data, analysis and interpretation of data, statistical analysis, drafting of manuscript.
SI: Acquisition of data, analysis and interpretation of data, critical revision of manuscript
SA: Acquisition of data, critical revision of manuscript
YZ: Acquisition of data, technical and material support, critical revision of manuscript
LW: Acquisition of data, technical and material support.
MZ: Technical and material support, critical revision of manuscript
MKH: Critical revision of manuscript and editing
PG: Technical and material support, critical revision of manuscript
BX: Technical and material support, critical revision of manuscript
DM: Study concept and design, obtained funding, study supervision, critical revision of manuscript.

revealed an increased expression of PepT1 in patients with colorectal cancer, suggesting that PepT1 might be targeted for the treatment of CAC. The use of an anti-inflammatory tripeptide KPV (Lys-Pro-Val) transported by PepT1 was able to prevent carcinogenesis in WT mice. When administered to PepT1-KO mice, KPV did not trigger any of the inhibitory effect on tumorigenesis observed in WT mice.

Conclusions—The observations that pepT1 was highly expressed in human colorectal tumor and that its overexpression and deletion in mice increased and decreased colitis associated tumorigenesis, respectively, suggest that PepT1 is a potential therapeutic target for the treatment of colitis associated tumorigenesis.

Keywords

Colitis-associated cancer; Intestinal inflammation; PepT1; KPV peptide

Introduction

The Proton-dependent Oligopeptide Transporter (POT) family includes four transporter proteins belonging to the SLC15A solute carrier group [1]. Of them, PepT1 is a di- and tripeptide transporter that is primarily expressed in the small intestine of healthy individuals. PepT1 transports di/tripeptides from the lumen into epithelial cells *via* an inward-directed proton gradient [2]. Under normal physiological condition, intestinal epithelial cells show apical expression of PepT1, facilitating the transport and absorption of di/tripeptides from endogenous sources in the small intestinal epithelial cells. There are some controversies regarding whether PepT1 is also expressed in colonic tissues. Multiple studies have reported little or no PepT1 expression at mRNA levels in the colons of healthy humans and rodents [3–10]. Other reports have suggested that PepT1 mRNAs were regionally distributed in the colon, with little or no expression in proximal colon and an increased expression in the distal colon [5, 6, 11]. While another study showed PepT1 protein expression using immunofluorescence in the proximal colon at steady state, the potential transport functions of colonic PepT1 was not investigated[11].

Despite these controversies regarding pepT1 expression during steady state, the alterations to expression profile of PepT1 within the gastrointestinal tract during chronic inflammation have been well described. In patients with chronic diseases, such as inflammatory bowel disease (IBD) and short bowel syndrome, PepT1 expression is upregulated in the colon [7, 12]. Colonic PepT1 is highly expressed in $IL10^{-/-}$ mice with colitis but not in *Lactobacillus plantarum* treated $IL10^{-/-}$ mice, lacking any signs of colitis [13]. It was also shown that colonic PepT1 expression and function may be induced in mice under pathological conditions of the colon from *Citrobacter rodentium* infection [14]. In addition to di/tripeptides from the diet and other endogenous sources, PepT1 is also able to transport di/tripeptides from bacterial origin, such as N-formyl-methionine-leucine-phenylalanine (fMLP) [15–20], muramyl dipeptide (MDP) [21], and L-Ala-gamma-D-Glu-mDAP (Tri-DAP) [22]. Previous *in vitro* results from our laboratory and others have demonstrated that bacterial peptide transport by PepT1 in colonic epithelial cells could trigger downstream pro-inflammatory events, including increased production of inflammatory cytokines *via* NF-κB pathway activation, and deregulation of colonic miRNA expression [17, 21–23]. These findings suggest

that PepT1 could play a crucial role in cell-to-cell communication during colitis. In the context of IBD, a functional *hPepT1* SNP (rs2297322) was recently linked to the presence of IBD in Swedish patients free of the NOD2 mutations [24], suggesting that *hPepT1* mutation may contribute to the pathology of IBD. However, additional studies are needed to explore how this mutation affects the expression and function of PepT1 during IBD.

In two previous studies [18, 25], we designed transgenic (TG) mice that overexpressed PepT1 under the control of the *villin* promoter (which confers specific expression in intestinal epithelial cells) and obtained PepT1-KO mice from Deltagene (San Mateo, CA), in order to examine how PepT1 overexpression or deletion affected intestinal inflammation using various models of colitis. Our results demonstrated that overexpression of PepT1 in intestinal epithelial cells increased inflammation and exacerbated colitis pathology [25]. In Dextran sodium sulfate (DSS)-treated TG mice, the degree of pathology was correlated to increased pro-inflammatory cytokine production, increased neutrophil infiltration and greater weight loss compared to wild-type (WT) mice [25]. Importantly, DSS-treated PepT1-KO mice developed a moderate colitis compared to WT mice [26]. Histological examination revealed that DSS-treated PepT1-KO mice exhibited less of pro-inflammatory cytokine production, neutrophil infiltration and weight loss compared to DSS-treated WT mice. In addition, knockout of PepT1 decreased the chemotaxis of immune cells recruited to the intestine during inflammation. Finally, phenotypes observed with both TG and PepT1-KO mice were linked to the presence of gut microbiota since they were attenuated by antibiotic treatment [25, 26]. Together, these findings suggested that PepT1 expression in immune cells regulates the secretion of pro-inflammatory cytokines triggered by bacteria and/or bacterial products, thus playing an important role in the induction of colitis.

Colorectal cancer (CRC) is among the most common human malignancies [27] and has been firmly linked to chronic intestinal inflammation, giving rise to the term “colitis-associated cancer” (CAC) [7, 28]. The development of CAC in patients suffering from IBD is one of the best characterized examples of an association between intestinal inflammation and carcinogenesis [29–34]. Among patients with ulcerative colitis (UC), the risk of colon cancer has been found to be as high as 2% at 10 years, 8% at 20 years, and 18% at 30 years after initial diagnosis[29]. In contrast, the lifetime risk of sporadic colorectal cancer in the United States is only 5% [35]. In present study, we hypothesized that PepT1 could be involved in CAC development due to its role in intestinal inflammation. To test this hypothesis, we used both TG and PepT1-KO mice and employed a well-known murine model of CAC using the carcinogen, azoxymethane (AOM), followed by two cycles of DSS [36, 37]. PepT1 has been shown to transport many types of drugs/prodrugs [38–40], including KPV [41]. This anti-inflammatory tripeptide, which is derived from α-melanocyte stimulating hormone (α-MSH), has been shown to have anti-inflammatory properties [42, 43] and to effectively reduce chemically induced colitis in mice [41, 44, 45]. Therefore, we hypothesized that KPV may attenuate tumorigenesis in the AOM/DSS-induced murine model of colon cancer.

In this study, we reported the effect of PepT1 overexpression and deletion in AOM/DSS-induced carcinogenesis. We interestingly observed that KPV was able to decrease the tumor number and the proliferation of malignant colonic epithelial cells in a PepT1 dependent way,

confirming that PepT1 can be a therapeutic target for the treatment of colonic inflammation and subsequent tumorigenesis.

Methods

Mice

Eight-week old female TG, PepT1-KO and the respective WT mice with matching C57BL/6 or FVB/NJ background were used in this study. Apc^{Min} mice ($Apc^{Min/+}$) were purchased from the Jackson Laboratory (Bar Harbor, ME). Mice were housed in specific pathogen-free conditions and fed ad libitum. All the experiments involving mice were approved by institutional animal care and use committee (IACUC, Georgia State University Atlanta, GA, USA), permit number A14010, and A14007.

Colitis-associated cancer and intestinal adenoma spontaneous models

CAC was induced as previously described with some modifications [46]. Mice were intraperitoneally (IP) injected with AOM (10 mg/kg body weight) (Sigma-Aldrich, St. Louis, MO) diluted in PBS (10mg/kg) and maintained on regular diet and water for 5 days. Mice were then subjected to two cycles of DSS treatment (MP Biomedicals, Solon, OH, USA), in which each cycle consisted of 2.5% DSS for 7 days followed by a 14-day recovery period with regular water. Mice were sacrificed by CO^2 asphyxiation. Colonic tumors were counted and measured using a dissecting microscope. Colonic tumors were counted and grouped by size as follows: <1, 1–2, and >2mm. The total sum of the area of tumors for each colon was given as the tumor burden index.

In experiments testing the efficacy of KPV (Biopeptide Co. Inc., San Diego, CA) the above protocol was used with slight modifications. Five days after AOM injections (10mg/kg or 15mg/kg to WT or PepT1-KO, respectively), WT or PepT1-KO mice were given 3% DSS with or without KPV for seven days, followed by 14 days of normal drinking water, then 2.5% or 3% DSS in WT or PepT1-KO mice, respectively, with or without KPV for seven days followed by 14 days of normal drinking water. The KPV-treated group received 100 μM KPV in their drinking water along with the DSS during both DSS cycles. While receiving DSS treatment mice were weighed daily to ensure that mice did not lose greater than 20% of their original body weight.

From 5 weeks to 18 weeks of age, $APC^{Min/+}$ mice were treated with KPV diluted to 100μM in the drinking water. Mice were sacrificed at 18 weeks of age by CO^2 asphyxiation. The entire small intestine and colon were dissected longitudinally. Intestinal tissues were examined under a dissecting microscope and counted for the presence of adenomas. Intestinal adenomas were counted and grouped by size as follows: <1, 1–2, and >2mm.

Human Colon Tissue Microarray

Human colon tissue array slides were purchased from US Biomax, Inc. (Rockville, MD). The microarray slide consisted of 75 samples in duplicates of normal, reactive, and cancerous (different grades and stages) colon tissues. The grading system of the tumor was as follow: Grade 1 or well-differentiated (cells appear normal and are not growing rapidly);

Grade 2 or moderately-differentiated (cells appear slightly different than normal); Grade 3 or poorly differentiated (cells appear abnormal and tend to grow and spread more aggressively); Grade 4 or undifferentiated (features are unremarkably different from that of undifferentiated cancers of other organs). The previously described antibody against hPepT1 [7] was used to stain the array slides at US Biomax, Inc. (Rockville, MD) and subsequent imagings were performed by the employees of US Biomax, Inc., in which were then sent to our laboratory for the further analysis of epithelial hPepT1 staining (Rabbit h-PepT1, dilution 1:3000). Images were then scored according to two parameters (from 0 to 2): the intensity of the staining (0: absence of PepT1 positive cells, 1: low intensity staining, 2: High intensity staining) and the areas of positive cells in the epithelium (0: absence of PepT1 positive cell, 1: less than the half of the epithelium was PepT1 positive, 2: the half or more of the epithelium was PepT1 positive). The intensity was indexed by the surface parameter giving one final score for each slide.

H&E Staining of Colonic Tissue

Mouse colons were fixed in 10%-buffered formalin for 24 h at room temperature and then embedded in paraffin. Tissues were sectioned at 5-μm thickness and stained with hematoxylin & eosin (H&E) using standard protocols. Images were acquired using an Olympus microscope equipped with a DP-23 Digital camera.

Immunohistochemistry

Mouse colons were fixed in formalin and paraffin-embedded. For Ki67, β-catenin, and PepT1 staining, sections were deparaffinized. Sections were incubated in sodium citrate buffer (pH 6.0) and cooked in a pressure cooker for 10 minutes for antigen retrieval. Sections were then blocked with 5% goat serum in TBS followed by one hour incubation with anti-Ki67 (1:100, Vector Laboratories, Burlingame, CA), anti-β-catenin (1:1000, Cell Signaling, Danvers, MA) or anti-mPepT1 at 37° C. After washing with TBS, sections were treated with appropriate biotinylated secondary antibodies for 30 minutes at 37°C, and color development was performed using the Vectastain ABC kit (Vector Laboratories). Sections were then counterstained with hematoxylin, dehydrated, and coverslipped. Images were acquired using an Olympus microscope equipped with DP-23 Digital camera. Ki67-positive cells were counted per crypt.

Terminal deoxynucleotidyl transferase deoxyuridine triphosphate nick-end labeling (TUNEL) staining

To quantitate the number of apoptotic cells in colonic epithelial cells, paraffin sections were deparaffinized and stained for apoptotic nuclei according to the manufacturer's instructions using the *In Situ* Cell Death Detection Kit (Roche Diagnostics, Indianapolis, IN). Images were acquired using an Olympus microscope equipped with a Hamamatsu black and white ORCA-03G digital camera. TUNEL-positive cells that overlapped with DAPI nuclear staining were counted per crypt.

Cytokine expression levels

RNA Extraction and Real-Time RT-PCR Total RNA were extracted from colonic tissues using RNeasy mini Kit (Qiagen) according to the manufacturer's instructions. Yield and quality of RNA were verified with a Synergy 2 plate reader (BioTek, Winooski, VT, USA). cDNA were generated from the total RNA isolated above using the Maxima first-strand cDNA synthesis kit (Thermo Scientific, Lafayette, CO, USA). mRNA expression were quantified by quantitative real-time reverse transcription-PCR (qRT-PCR) using Maxima SYBR green/ROX (6-carboxyl-X-rhodamine) quantitative PCR (qPCR) Master Mix (Thermo Scientific) and the following sense and antisense primers: IL-6 5′-ACAAGTCGGAGGCTTAATTACACAT-3′ and 5′-TTGCCATTGCACAACTCTTTTC-3′; CXCL2 5′-CACTCTCAAGGGCGGTCAAA-3′ and 5′-TACGATCCAGGCTTCCCGGGT-3′; IL-22 5′-GTCAACCGCACCTTTATGCT-3′ and 5′-GTTGAGCACCTGCTTCATCA-3′; IL-10 5′-GGTTGCCAAGCCTTATCGGA-3′ and 5′-CTTCTCACCCAGGGAATTCA-3′; tumor necrosis factor α (TNF α) 5′-AGGCTGCCCCGACTACGT-3′ and 5′-GACTTTCTCCTGGTATGAGATAGCAAA-3′; 36B4 5′-TCCAGGCTTTGGGCATCA-3′ and 5′-CTTTATCAGCTGCACATCACTCAGA-3′. Results were normalized by using 36B4 housekeeping gene.

Western blot

Whole colon lysates were made by homogenizing a small piece of distal colon in Radio-Immunoprecipitation Assay (RIPA) buffer plus Halt phosphatase and protease inhibitor cocktail (Thermo Fisher Scientific Inc.). Fifty μg of lysate per well were resolved on polyacrylamide gradient gels and transferred to nitrocellulose membranes (Bio-Rad, Hercules, CA). Membranes were probed with relevant primary antibodies, including β-catenin, p-Iκκ-α/β and β-actin (Cell Signaling), mPepT-1, p-ERK1/2 and total ERK1/2 (Santa Cruz Biotechnology, Inc., Santa Cruz, CA) followed by incubation with appropriate HRP-conjugated secondary antibodies (GE Healthcare Biosciences, Pittsburgh, PA). Blots were developed using ECL Western Blotting Detection reagents (GE Healthcare Biosciences). Densitometry quantifications were performed using the software Quantity One (Bio-Rad).

Statistical Analysis

Data are presented as means ± SEM. Statistical analysis for significance was determined using ANOVA test followed by a Bonferroni post-test (GraphPad Prism). Differences were noted as significant: *P<0.05, **P<0.01 and ***P<0.001.

Results

Tumor growth is increased in mice that overexpress PepT1 in intestinal epithelial cells

We first examined if PepT1 overexpression in the colon could contribute to the development of CAC, as it was previously demonstrated that TG mice had increased inflammation and exacerbated pathologies during acute colitis [25]. Our laboratory previously generated TG mice that overexpress PepT1 under the control of the *villin* promoter [25], which is primarily

active in intestinal epithelial cells. When these mice were treated with AOM/DSS, they tended to develop an increased number of tumors compared to WT mice though this did not reach statistical significance (p= 0.06), reflecting an important variability between individuals (Figure 1A–1B). The number of large tumors (> 2 mm^2) was highly increased in TG versus WT mice (Figure 1C), as was the overall tumor burden index (i.e., the total area of tumors per colon) (Figure 1D), indicative of increased susceptibility to tumorigenesis in TG mice, with an enhanced tumor growth and/or tumor cell survival. Despite the absence of any difference in body weight loss between WT and TG mice during the AOM/DSS protocol (Figure 1E), the colon lengths were decreased in TG mice compared to WT mice treated by AOM/DSS, showing that the TG mice were more susceptible to colitis (Figure 1F). Histological examination revealed the presence of larger adenomas and increased areas of inflammatory cell infiltration (arrow) in colonic sections from AOM/DSS-treated TG and WT mice (Figure 1G), with increased dysplasia, aberrant crypt foci and cellular infiltration in the colonic epithelia of AOM/DSS-treated TG mice compared to WT mice. Histologically, we did not observe any difference between water-treated (control) TG and WT mice. Next, we determined the mRNA expression levels of pro-inflammatory cytokines and chemokines and found the levels of *Il-6*, *Cxcl2* and *Il-22* to be significantly higher in AOM/DSS-treated TG mice compared to treated WT mice (Figure 1H), supporting the previous observation that TG mice were more sensitive to intestinal inflammation and tumorigenesis induced by AOM/DSS treatment. Interestingly, the expression level of mRNA encoding TNF-α, a pro-inflammatory cytokine reported to have an increased expression in colitis and CAC [47], did not significantly differ between TG and WT mice (Figure 1H). The anti-inflammatory cytokine IL-10 expression was decreased in AOM/DSS-treated TG mice compared to similarly treated WT mice (Figure 1H). In control (water-treated) TG and WT mice, no significant difference of these cytokine levels were observed (Figure 1H). Taken together, these data indicate that TG mice are more susceptible to AOM/DSS treatment than WT mice, suggesting a potential role of PepT1 in the initiation and exacerbation of cancer development.

Overexpression of hPepT1 deregulates proliferation and apoptosis

The increase in tumor burden and average tumor size in TG mice suggested that they may be subjected to increased cell proliferation compared to WT mice. Proliferation of the colonic epithelial cells was analyzed using an antibody against the nuclear marker Ki67. No significant difference in the cellular proliferation between water-treated WT and TG mice was observed (Figure 2A–B). However, following AOM/DSS treatment, the number of Ki67 positive cells was increased in both WT and TG mice, but to a significantly higher level in TG mice compared to WT mice (Figure 2A–B). This observation indicates that overexpression of PepT1 in intestinal epithelial cells exacerbate the AOM/DSS-induced proliferation of crypt cells in the colonic epithelium. Ki67-positive cells were highly prevalent in the colon tumors of both WT and TG mice (data not shown). In addition, a TUNEL-based quantification of apoptosis in colonic sections from WT and TG mice revealed that the epithelia of AOM/DSS-treated WT mice had significantly more TUNEL+ cells compared to treated TG mice (Figure 2C–D). While AOM/DSS treatment increased the number of apoptotic cells in both WT and TG mice, the fold change was significantly higher in the former (Figure 2D), indicating that PepT1 overexpression in epithelial cells

minimized AOM/DSS-induced apoptosis in the colonic epithelia. Together, these data demonstrated that PepT1 overexpression in intestinal epithelia may induce various pathways that lead to increased proliferation and/or decreased apoptosis of colonic epithelial cells, thereby potentially contributing to the increased tumor burden observed in TG mice.

Overexpression of hPepT1 alters tumorigenesis signaling pathways

Several signaling pathways have been associated with the regulation of tumorigenesis in the AOM/DSS CAC mouse model and human CAC. Among them, β-catenin is an oncogenic protein that plays important roles in cell adhesion and in a co-transcriptional activation of genes of the Wnt signaling pathway (e.g., *c-myc, cyclooxygenase-2, metalloproteinase-7* and *cyclin D1*) [48]. AOM induces mutations of β-catenin at specific serine and threonine residues that are targeted by GSK-3β phosphorylation, leading to the cellular accumulation of β-catenin [36]. β-catenin immunohistochemical staining demonstrated that the levels of free β-catenin were increased in the cytoplasm of tumor cells from AOM/DSS-treated WT and TG mice compared to control (water-treated) animals, where the majority of β-catenin staining was associated with the cellular membranes (Figure 2E). We also observed an increased nuclear accumulation of β-catenin in tumor cells from TG mice compared to WT mice (Figure 2E), suggesting that the transcription of β-catenin may be enhanced in these cells. Consistent with these results, AOM/DSS-treated WT and TG mice had increased levels of β-catenin compared to their water-treated counterparts, and β-catenin expression was slightly higher in colon lysates from TG mice compared to WT mice as shown in densitometric analysis of Western Blot (Figure 2F–G). The NF-κB and MAPK pathways have also been implicated in colon tumorigenesis [36, 49], so we next examined associated signaling partners of these pathways by Western blot. Levels of phosphorylated Iκκ-α/β and phosphorylated IκB-α were highly increased in AOM/DSS-treated TG mice, but only marginally in comparably treated WT mice (Figure 2F–G), suggesting that NF-κB signaling is enhanced in AOM/DSS-treated TG mice compared to WT mice. Finally, we observed increased levels of phosphorylated ERK1/2 in AOM/DSS-treated WT and TG mice compared to their respective water controls (Figure 2F–G) but found no significant AOM/DSS treatment effect between the two genotypes, suggesting that this pathway was not be required for the increased tumor growth observed in PepT1 TG mice.

Decreased tumorigenesis in PepT1-deficient mice

Next, we investigated whether the absence of PepT1 could protect from AOM/DSS-induced CAC phenotype. Following AOM/DSS-treatment, PepT1-KO mice developed significantly fewer tumors (of all sizes) compared to similarly treated WT mice (Figure 3A–C). Consistent with these data, the overall tumor burden was significantly lower in AOM/DSS-treated PepT1-KO mice compared to AOM/DSS-treated WT mice (Figure 3D). These data suggest that, in absence of PepT1, mice were protected from tumor initiation and growth. Since intestinal inflammation is known to be a central factor in the initiation and development of colon tumors, we next measured various parameters of inflammation after the induction of CAC in WT and PepT1-KO mice. Monitoring of body weight showed that WT mice underwent a dramatic weight loss during the first cycle of DSS, whereas no such effect was observed in PepT1-KO mice (Figure 3E). The colons were longer in PepT1-KO AOM/DSS treated compared to the WT counterpart confirming that the PepT1-KO mice

were more resistant to colitis than WT mice (Figure 3F). Histological examination revealed the presence of large adenomas with major lymphocyte infiltration in colonic sections from AOM/DSS-treated WT mice (Figure 3G), whereas no lymphocyte infiltration or adenoma was detected in AOM/DSS-treated PepT1-KO mice (Figure 3G). We did not observe any difference of these parameters between control (water-treated) PepT1-KO and WT mice (Figure 3G). Next, we examined the mRNA levels of pro-inflammatory cytokines and chemokines in WT and PepT1-KO mice with or without CAC induction. We found that the expression levels of *Il-6*, *Cxcl2*, *Il-22* and *Tnf-α* were significantly increased in WT mice after AOM/DSS treatment. Importantly, while *Il-6* and *Cxcl-2* were only moderately elevated in AOM/DSS-treated PepT1-KO mice, level of *Il-22* and *Tnf-α* were significantly elevated (Figure 3H). The expression level of *Il-10* in PepT1-KO mice tended to be lower than that in WT mice, but no significant difference was observed regardless of the genotype or treatment (Figure 3H). These results showed that AOM/DSS-associated intestinal inflammation was attenuated in PepT1-KO mice compared to WT mice.

Taken together, these data indicate that PepT1-KO mice were protected against AOM/DSS-induced tumorigenesis through a partial inhibition of tumorigenic intestinal inflammation. This supports our hypothesis that PepT1 play a central role in the initiation and exacerbation of CAC in mice.

PepT1-KO mice elicit a beneficial balance of proliferation and apoptosis in the colonic mucosa associated with inhibition of tumorigenesis-related signaling

Ki67 staining demonstrated that there was no significant difference in cellular proliferation among water-treated (control) WT and PepT1 mice as well as AOM/DSS-treated PepT1-KO mice, whereas AOM/DSS-treated WT mice had significantly more Ki67 positive cells per crypt (Figure 4A–B). This indicates that, in the absence of PepT1, proliferation of crypt epithelial cells was inhibited. Importantly, Ki67 positive cells were located in the entire crypt in WT mice, while they were located only in basal crypts in PepT1KO mice attesting the extensive proliferation occurring in WT mice when subjected to AOM/DSS. Next, we used TUNEL staining to determine the levels of apoptosis in colonic mucosa sections from WT and PepT1-KO mice. The basal level of apoptosis was slightly but significantly higher in PepT1-KO mice compared to WT mice, and the number of apoptotic cells in the epithelia of WT and (to a lesser extent) PepT1-KO mice was significantly greater after AOM/DSS treatment (Figure 4C–D). Thus, PepT1 deficiency appears to be protective against the proliferative and abnormal apoptosis status induced by AOM/DSS treatment.

In order to investigate whether PepT1 deficiency inhibits tumorigenesis signaling pathways, the accumulation of proteins involved in tumorigenesis was analyzed by Western-blot. Increased levels of phosphorylated Iκκ-α/β were observed in AOM/DSS-treated PepT1-KO mice compare to AOM/DSS-treated WT mice, whereas no difference was observed in the levels of phosphorylated IκB-α and total IκB-α between the two genotypes (Figure 4E–F), suggesting that the inhibition of NF-κB pathway was not the mechanism underlying the attenuated tumor growth associated with PepT1 deficiency. Compared to the relevant controls, β-catenin levels were unaltered in AOM/DSS-treated WT mice and comparably treated PepT1-KO mice, whereas the levels of phosphorylated ERK1/2 were drastically

increased in AOM/DSS-treated WT mice but remained unchanged in AOM/DSS-treated PepT1-KO mice (Figure 4E–F). This finding suggests that PepT1 deficiency may antagonize and/or protect from the AOM/DSS-induced ERK pathway. Together, these results suggest that inhibition of the tumor-growth-promoting ERK pathway [50, 51] might be involved in the inhibition of AOM/DSS-associated tumor growth observed in PepT1-KO mice.

KPV prevents intestinal inflammation and tumorigenesis during colitis-associated carcinogenesis in a PepT1 dependent manner

The analysis of PepT1 expression at the mRNA and proteins levels both indicated that PepT1 levels were upregulated in the colons of AOM/DSS-treated WT mice (Figure 5A and 5C). WT mice treated with AOM/DSS had increased PepT1 staining in epithelial cells lining the colon compared to water-treated (control) mice (Figure 5B). These immunohistochemical data were further verified by Western blot analysis of whole-colon lysates (Figure 5C), where greater PepT1 expression was found in the colon of AOM/DSS-treated WT animals. Therefore, we predicted that colonic PepT1 would be also upregulated in colon cancer patients, as previously described for bladder cancer specimens at mRNA levels [52]. To determine if PepT1 was upregulated during human disease, we analyzed a human tissue microarray, stained for hPepT1, that included paraffin-embedded samples from control patients and colon cancer patients with various stages of malignancies from Grade I to Grade III, as well as patients with benign colon tumors (male and female patients ranging in age from 19 to 92). The images were then analyzed and scored for epithelial/tumor cell hPepT1 staining. Most of the colon cancer patients demonstrated hPepT1 staining in their epithelial and/or tumor cells (Figure 6 A–B). In normal colon samples, some hPepT1 staining was observed in cells surrounding the epithelium, which are most likely immune cells [16]. In the benign colon adenoma, hPepT1 staining was observed in limited areas of epithelia, probably as a consequence of inflammation, as previously reported [7]. Importantly, the majority of the colon tumor samples showed increased staining relative to both normal and benign tissues (Figure 6B). The specific up-regulation of PepT1 in tumor tissues reveals the potential use of PePT1 transporter activity in the treatment of CAC.

Several studies have previously shown that KPV tri-peptide decreased intestinal inflammation and attenuated DSS-induced colitis [41, 44, 45], suggesting tripeptide as a valuable therapeutic tool against colitis and associate carcinogenesis. We previously demonstrated that KPV was transported *via* PepT1 *in vitro* in Caco-2/BBE cells [41]. We then hypothesized that KPV may help to prevent colon tumorigenesis in the AOM/DSS-induced CAC model. To test this hypothesis, WT mice were treated with AOM/DSS or AOM/DSS + KPV, revealing that WT mice given KPV in conjunction with AOM/DSS exhibited drastic decrease in colon tumorigenesis, as revealed by tumor numbers, sizes, and overall colonic tumor burdens (Figure 7A–D), compare to AOM/DSS-treated-only animals. While both groups of mice lost similar amounts of weight during DSS treatment (Figure 7E), KPV-treated mice exhibited decreased inflammation, fewer aberrant crypt foci, decreased cellular infiltration (as seen on H&E-stained sections), and less epithelial cell proliferation (i.e., fewer $Ki67^+$ cells/crypts) (Figure 7F–H). In order to investigate putative protective effect of KPV administration in PepT1-KO mice, colitis-associated cancer protocol was slightly modified based on the relative low penetrance of the disease in PepT1-deficient animals

(Figure 3). AOM concentration was increased to 15mg/kg and DSS to 3% in order to favor tumor development. We observed that, unlike WT mice, PepT1-KO animals were not protected from tumorigenesis by KPV administration, as revealed by tumor numbers, sizes, and tumor burden that were not significantly changed between AOM/DSS and AOM/DSS + KPV groups (Figure 8A–D). Despite the statistical non-significance, a trend for a decreased tumor burden index was seen in KPV treated group. These data importantly reveal that KPV acts at least in part through PepT1, opening an important potential therapeutic avenue for the treatment of colonic inflammation and subsequent tumorigenesis.

KPV was shown to decrease tumorigenesis in a colitis-associated model of cancer. We next wanted to know whether KPV would also reduce tumorigenesis in a non-inflammatory model. For this purpose, $APC^{Min/+}$ mice, a genetic model of intestinal adenocarcinoma that spontaneously develops adenomas mainly in the small intestine, were treated with KPV for 13 weeks. As presented in Figure 9, KPV did not decrease the tumor burden in the small intestine nor in the colon. However, our results importantly showed that intestinal inflammation, assessed by Lipocalin-2 (Lcn-2) measurement, was decreased by KPV treatment, confirming the anti-inflammatory effect of KPV in this model. Those results indicated that the decrease of intestinal inflammation induced by KPV, observed in Figure 7, was not sufficient to decrease the tumor formation in a genetic model of tumorigenesis. However, genetic colon carcinoma models only represent 2–5% of all colon cancers [53] and have a severe tumor development even in germ free mice and a dramatically decreased basal intestinal inflammation [54]. Therefore, although the inhibition of intestinal inflammation *via* KPV/PepT1 pathway was not sufficient to inhibit tumorigenesis in such a stringent model as the $APC^{Min/+}$ mice, KPV revealed a promising potential for inhibiting the inflammation in various models of colon cancer.

Discussion

The present study demonstrates that PepT1 overexpression leads to increased inflammation and colonic tumor burdens in a murine model of CAC, strongly suggesting that PepT1 plays a crucial role in CAC. Previous reports showed that PepT1 protein expression was upregulated in colon under the conditions of chronic inflammation, such as IBD [7, 28]; this may increase the interactions between bacterial peptides and intracellular innate immune receptors (e.g., NOD receptors), thereby triggering the downstream activation of pro-inflammatory signaling pathways [25, 55].

In TG mice, we observed upregulation of pro-inflammatory cytokines/chemokines and downregulation of an anti-inflammatory cytokine (IL-10) compared to WT mice. It has been reported that IL-10-deficient mice develop spontaneous colitis, and after 3 and 6 months, 25% and 60% of the mice develop adenocarcinomas, respectively[56]. Thus, IL-10 appears to play an important role in intestinal inflammation. Interestingly, colonic PepT1 protein was expressed in $IL\text{-}10^{-/-}$ mice that show signs of colitis, but not in non-colitic $IL10^{-/-}$ mice [13], suggesting that PepT1 contributes to the development of colitis in this model. In IL-10-deficient mice, tumorigenesis was decreased by the administration of exogenous IL-10, even after colitis had developed [32, 56]. Following the induction of the CAC tumor model, we herein found that PepT1-overexpressed TG mice had increased inflammation, larger tumors

and greater overall tumor burdens compared to WT mice, suggesting that PepT1 expression in intestinal epithelial cells may enhance tumor cell growth or survival in the presence of a carcinogenic assault (here, AOM/DSS treatment). Despite the non-significance (p=0.06), a trend for an increased tumor number was observed in TG mice subjected to AOM/DSS treatment compared to WT. The observation of a subtle increase suggested that the tumor initiation was not the main process being affected by PepT1. Instead, PepT1 appears to enhance the proliferation/survival of tumor cells, contributing to the presence of larger tumors throughout the colon. Consistent with this hypothesis, cell proliferation was increased while apoptosis was decreased in the epithelial crypts of TG mice. The tumor number was significantly lower in PepT1-KO mice than WT mice, however, suggesting that different pathways are involved in the protective effect observed in PepT1-KO mice *versus* the aggravating effect observed in TG mice. To test this hypothesis, we used Western blot to examine various proteins involved in the pro-survival, proliferation and tumorigenesis signaling pathways. AOM/DSS treatment enhanced the activation of the NF-κB and Wnt/β-catenin pathways in TG mice compared to WT mice, but no such change was seen in PepT1-KO mice. Conversely, phosphorylated ERK1/2 was similarly upregulated following AOM/DSS treatment of TG and WT mice, but this upregulation was abrogated in PepT1-KO mice. This suggests that the absence of PepT1 inhibits the ERK pathway, potentially explaining (at least in part) the inhibition of tumor development and growth observed in PepT1-KO mice.

Since colonic PepT1 is expressed at minimal levels in healthy individuals, treatments that effectively downregulate PepT1 expression in IBD or, as shown in our study, in CAC patients where PepT1 is expressed at higher levels, may attenuate inflammation and reduce the risk for tumorigenesis. For example, treatment of IL-$10^{-/-}$ mice with the probiotic, *Lactobacillus plantarum*, reduced PepT1 expression and activity and attenuated colitis compared to vehicle-treated IL-$10^{-/-}$ animals [57]. Alternatively, since we showed that PepT1 was upregulated in colons of mice with AOM/DSS-induced CAC and in human colon adenocarcinoma, treatments that exploit the transporter activity of PepT1 could increase the effectiveness of particular drugs by enhancing their bioavailability after oral administration. PepT1 transports several types of peptide-derived drugs, including antibiotics, inhibitors of angiotensin-converting enzyme, and anti-cancer and anti-viral drugs [38, 39, 58]. Among them, the PepT1 substrate and anti-tumor drug, bestatin, was found to decrease cell proliferation, ameliorate tumor growth [59], inhibit the growth of colon adenocarcinoma, and decrease the growth of myeloid leukemia C1498 cells *in vivo* [60]. In this study, we specifically focused on another peptide, namely KPV.

KPV, a tripeptide from the C-terminus of α-melanocyte-stimulating hormone, confers anti-inflammatory effects [61, 62]; acting as a substrate for and actively transported by PepT1 *in vitro* [41]. Following stimulation with pro-inflammatory cytokines, Caco2-BBE and Jurkat cells that were co-treated with KPV showed attenuated NF-κB activation and decreased pro-inflammatory cytokine production [41]. Our data presented here, importantly demonstrate that KPV treatment is able to decrease AOM/DSS induced tumorigenesis. This was occurring in a PepT1 dependent manner, since PepT1-KO animals were not protected from tumorigenesis by KPV administration. However, a trend for a decreased tumor burden index was still seen in PepT1-KO in KPV treated group compared to the water control group, pointing that, even

if mainly PepT1 dependent, KPV might also be transported by other peptide transporters. KPV still represents a promising drug for targeting PepT1, as inferred from a previous study that found a high affinity of hPepT1 for KPV (Km~160μM) in Caco2-BBE cells [41]. This Km is among the lowest Kms reported for hPepT1. For example, Gly-Sar, which is the most commonly used PepT1 substrate, has a Km ≥ 1 mM in Caco2-BBE cells [63]. This will allow low doses of KPV to be efficiently transported by PepT1. This aspect is of high interest for using this tri-peptide in clinic for the treatment of IBD or CAC.

IBD-related inflammation is believed to increase the risk of colorectal cancer, but many existing studies have failed to show strong positive link between the anti-inflammatory drugs commonly used to treat IBD and a decreased risk of colon cancer [64]. However, a long-term reduction of the inflammation by the use of NSAID was previously associated with a protective role against colorectal cancer [65]. In the present study, we reported a time-dependent increase of intestinal inflammation in $APC^{Min/+}$. Importantly, even with a limited inhibition of tumorigenesis in such a stringent model, KPV was sufficient to decrease the inflammation in this model of non-inflammatory-induced carcinogenesis. Therefore, we anticipate that the use of KPV prior to the development of colon cancer might be of interest as a preventive agent to the colonic carcinogenesis.

Overall, additional studies are warranted to determine the precise mechanism by which KPV decreases tumorigenesis in this model, and to test whether this tripeptide could be beneficial against human CAC.

Finally, several studies have shown that PepT1 is expressed by cancer cell types beyond colorectal cancer cells [66–68], including gastric and pancreatic cancer cells. Thus, the transporter activity of PepT1 either in small or large intestine may be used to address these other types of cancer, and future studies may identify other tumor types that display increased PepT1 expression.

Acknowledgments

Grant support: This work was supported by grants from the Department of Veterans Affairs (BX002526) and the National Institutes of Health of Diabetes and Digestive and Kidney (RO1-DK-071594 to D.M). E. Viennois is the recipient of a Research Fellowship Award from the Crohn's & Colitis Foundation of America. D. Merlin is a recipient of a Research Career Scientist Award from the Department of Veterans Affairs.

Abbreviations

AOM	azoxymethane
CAC	Colitis-associated-cancer
DSS	Dextran sodium sulfate
ERK	Extracellular signal-regulated kinases
IBD	Inflammatory Bowel Disease
IL10	Interleukin-10

IκB-α	inhibitor of kappa B
Iκκ-α/β	IκB kinase
KPV	Lys-Pro-Val
mRNA	messenger Ribonucleic acid
NF-κB	nuclear factor kappa-light-chain-enhancer of activated B cells
PCR	Polymerase chain reaction
PepT1	peptide transporter 1
TG	Transgenic
TUNEL	Terminal deoxynucleotidyl transferase dUTP nick end labeling
WT	Wild-type

References

1. Daniel H, Kottra G. The proton oligopeptide cotransporter family SLC15 in physiology and pharmacology. Pflugers Archiv: European journal of physiology. 2004; 447:610–8. [PubMed: 12905028]
2. Ingersoll SA, Ayyadurai S, Charania MA, Laroui H, Yan Y, Merlin D. The role and pathophysiological relevance of membrane transporter PepT1 in intestinal inflammation and inflammatory bowel disease. Am J Physiol Gastrointest Liver Physiol. 2012; 302:G484–92. [PubMed: 22194420]
3. Drozdzik M, Groer C, Penski J, Lapczuk J, Ostrowski M, Lai Y, Prasad B, Unadkat JD, Siegmund W, Oswald S. Protein Abundance of Clinically Relevant Multidrug Transporters along the Entire Length of the Human Intestine. Molecular pharmaceutics. 2014; 11:3547–55. [PubMed: 25158075]
4. Englund G, Rorsman F, Ronnblom A, Karlbom U, Lazorova L, Grasjo J, Kindmark A, Artursson P. Regional levels of drug transporters along the human intestinal tract: co-expression of ABC and SLC transporters and comparison with Caco-2 cells. European journal of pharmaceutical sciences: official journal of the European Federation for Pharmaceutical Sciences. 2006; 29:269–77. [PubMed: 16822659]
5. Jappar D, Wu SP, Hu Y, Smith DE. Significance and regional dependency of peptide transporter (PEPT) 1 in the intestinal permeability of glycylsarcosine: in situ single-pass perfusion studies in wild-type and Pept1 knockout mice. Drug metabolism and disposition: the biological fate of chemicals. 2010; 38:1740–6. [PubMed: 20660104]
6. Meier Y, Eloranta JJ, Darimont J, Ismair MG, Hiller C, Fried M, Kullak-Ublick GA, Vavricka SR. Regional distribution of solute carrier mRNA expression along the human intestinal tract. Drug metabolism and disposition: the biological fate of chemicals. 2007; 35:590–4. [PubMed: 17220238]
7. Merlin D, Si-Tahar M, Sitaraman SV, Eastburn K, Williams I, Liu X, Hediger MA, Madara JL. Colonic epithelial hPepT1 expression occurs in inflammatory bowel disease: transport of bacterial peptides influences expression of MHC class 1 molecules. Gastroenterology. 2001; 120:1666–79. [PubMed: 11375948]
8. Ogihara H, Saito H, Shin BC, Terado T, Takenoshita S, Nagamachi Y, Inui K, Takata K. Immuno-localization of H+/peptide cotransporter in rat digestive tract. Biochemical and biophysical research communications. 1996; 220:848–52. [PubMed: 8607854]
9. Ziegler TR, Fernandez-Estivariz C, Gu LH, Bazargan N, Umeakunne K, Wallace TM, Diaz EE, Rosado KE, Pascal RR, Galloway JR, Wilcox JN, Leader LM. Distribution of the H+/peptide transporter PepT1 in human intestine: up-regulated expression in the colonic mucosa of patients

with short-bowel syndrome. The American journal of clinical nutrition. 2002; 75:922–30. [PubMed: 11976168]

10. Ma K, Hu Y, Smith DE. Influence of fed-fasted state on intestinal PEPT1 expression and in vivo pharmacokinetics of glycylsarcosine in wild-type and Pept1 knockout mice. Pharmaceutical research. 2012; 29:535–45. [PubMed: 21904935]
11. Wuensch T, Schulz S, Ullrich S, Lill N, Stelzl T, Rubio-Aliaga I, Loh G, Chamaillard M, Haller D, Daniel H. The peptide transporter PEPT1 is expressed in distal colon in rodents and humans and contributes to water absorption. American journal of physiology Gastrointestinal and liver physiology. 2013; 305:G66–73. [PubMed: 23660505]
12. Ziegler TR, Fernandez-Estivariz C, Gu LH, Bazargan N, Umeakunne K, Wallace TM, Diaz EE, Rosado KE, Pascal RR, Galloway JR, Wilcox JN, Leader LM. Distribution of the H+/peptide transporter PepT1 in human intestine: up-regulated expression in the colonic mucosa of patients with short-bowel syndrome. Am J Clin Nutr. 2002; 75:922–30. [PubMed: 11976168]
13. Chen HQ, Yang J, Zhang M, Zhou YK, Shen TY, Chu ZX, Hang XM, Jiang YQ, Qin HL. Lactobacillus plantarum ameliorates colonic epithelial barrier dysfunction by modulating the apical junctional complex and PepT1 in IL-10 knockout mice. American journal of physiology Gastrointestinal and liver physiology. 2010; 299:G1287–97. [PubMed: 20884889]
14. Nguyen HT, Dalmasso G, Powell KR, Yan Y, Bhatt S, Kalman D, Sitaraman SV, Merlin D. Pathogenic bacteria induce colonic PepT1 expression: an implication in host defense response. Gastroenterology. 2009; 137:1435–47. e1–2. [PubMed: 19549526]
15. Merlin D, Steel A, Gewirtz AT, Si-Tahar M, Hediger MA, Madara JL. hPepT1-mediated epithelial transport of bacteria-derived chemotactic peptides enhances neutrophil-epithelial interactions. J Clin Invest. 1998; 102:2011–8. [PubMed: 9835627]
16. Charrier L, Driss A, Yan Y, Nduati V, Klapproth JM, Sitaraman SV, Merlin D. hPepT1 mediates bacterial tripeptide fMLP uptake in human monocytes. Lab Invest. 2006; 86:490–503. [PubMed: 16568107]
17. Buyse M, Tsocas A, Walker F, Merlin D, Bado A. PepT1-mediated fMLP transport induces intestinal inflammation in vivo. Am J Physiol Cell Physiol. 2002; 283:C1795–800. [PubMed: 12419711]
18. Shi B, Song D, Xue H, Li J, Li N. Abnormal expression of the peptide transporter PepT1 in the colon of massive bowel resection rat: a potential route for colonic mucosa damage by transport of fMLP. Digestive diseases and sciences. 2006; 51:2087–93. [PubMed: 17009119]
19. Wang P, Lu YQ, Wen Y, Yu DY, Ge L, Dong WR, Xiang LX, Shao JZ. IL-16 induces intestinal inflammation via PepT1 upregulation in a pufferfish model: new insights into the molecular mechanism of inflammatory bowel disease. Journal of immunology. 2013; 191:1413–27.
20. Wu SP, Smith DE. Impact of intestinal PepT1 on the kinetics and dynamics of N-formyl-methionyl-leucyl-phenylalanine, a bacterially-produced chemotactic peptide. Molecular pharmaceutics. 2013; 10:677–84. [PubMed: 23259992]
21. Vavricka SR, Musch MW, Chang JE, Nakagawa Y, Phanvijhitsiri K, Waypa TS, Merlin D, Schneewind O, Chang EB. hPepT1 transports muramyl dipeptide, activating NF-kappaB and stimulating IL-8 secretion in human colonic Caco2/bbe cells. Gastroenterology. 2004; 127:1401–9. [PubMed: 15521010]
22. Dalmasso G, Nguyen HT, Charrier-Hisamuddin L, Yan Y, Laroui H, Demoulin B, Sitaraman SV, Merlin D. PepT1 mediates transport of the proinflammatory bacterial tripeptide L-Ala-{gamma}-D-Glu-meso-DAP in intestinal epithelial cells. Am J Physiol Gastrointest Liver Physiol. 2010; 299:G687–96. [PubMed: 20558765]
23. Ayyadurai S, Charania MA, Xiao B, Viennois E, Zhang Y, Merlin D. Colonic miRNA expression/secretion, regulated by intestinal epithelial PepT1, plays an important role in cell-to-cell communication during colitis. PloS one. 2014; 9:e87614. [PubMed: 24586284]
24. Zucchelli M, Torkvist L, Bresso F, Halfvarson J, Hellquist A, Anedda F, Assadi G, Lindgren GB, Svanfeldt M, Janson M, Noble CL, Pettersson S, Lappalainen M, Paavola-Sakki P, Halme L, Farkkila M, Turunen U, Satsangi J, Kontula K, Lofberg R, Kere J, D'Amato M. PepT1 oligopeptide transporter (SLC15A1) gene polymorphism in inflammatory bowel disease. Inflammatory bowel diseases. 2009; 15:1562–9. [PubMed: 19462432]

25. Dalmasso G, Nguyen HT, Ingersoll SA, Ayyadurai S, Laroui H, Charania MA, Yan Y, Sitaraman SV, Merlin D. The PepT1-NOD2 signaling pathway aggravates induced colitis in mice. Gastroenterology. 2011; 141:1334–45. [PubMed: 21762661]
26. Ayyadurai S, Charania MA, Xiao B, Viennois E, Merlin D. PepT1 expressed in immune cells has an important role in promoting the immune response during experimentally induced colitis. Laboratory investigation; a journal of technical methods and pathology. 2013; 93:888–99. [PubMed: 23797361]
27. Weir HK, Thun MJ, Hankey BF, Ries LA, Howe HL, Wingo PA, Jemal A, Ward E, Anderson RN, Edwards BK. Annual report to the nation on the status of cancer, 1975–2000, featuring the uses of surveillance data for cancer prevention and control. J Natl Cancer Inst. 2003; 95:1276–99. [PubMed: 12953083]
28. Wojtal KA, Eloranta JJ, Hruz P, Gutmann H, Drewe J, Staumann A, Beglinger C, Fried M, Kullak-Ublick GA, Vavricka SR. Changes in mRNA expression levels of solute carrier transporters in inflammatory bowel disease patients. Drug metabolism and disposition: the biological fate of chemicals. 2009; 37:1871–7. [PubMed: 19487253]
29. Eaden JA, Abrams KR, Mayberry JF. The risk of colorectal cancer in ulcerative colitis: a meta-analysis. Gut. 2001; 48:526–35. [PubMed: 11247898]
30. Ahmadi A, Polyak S, Draganov PV. Colorectal cancer surveillance in inflammatory bowel disease: the search continues. World J Gastroenterol. 2009; 15:61–6. [PubMed: 19115469]
31. Feagins LA, Souza RF, Spechler SJ. Carcinogenesis in IBD: potential targets for the prevention of colorectal cancer. Nat Rev Gastroenterol Hepatol. 2009; 6:297–305. [PubMed: 19404270]
32. Ullman TA, Itzkowitz SH. Intestinal inflammation and cancer. Gastroenterology. 2011; 140:1807–16. [PubMed: 21530747]
33. Ekbom A, Helmick C, Zack M, Adami HO. Increased risk of large-bowel cancer in Crohn's disease with colonic involvement. Lancet. 1990; 336:357–9. [PubMed: 1975343]
34. Jess T, Gamborg M, Matzen P, Munkholm P, Sorensen TI. Increased risk of intestinal cancer in Crohn's disease: a meta-analysis of population-based cohort studies. The American journal of gastroenterology. 2005; 100:2724–9. [PubMed: 16393226]
35. Thorsteinsdottir S, Gudjonsson T, Nielsen OH, Vainer B, Seidelin JB. Pathogenesis and biomarkers of carcinogenesis in ulcerative colitis. Nat Rev Gastroenterol Hepatol. 2011; 8:395–404. [PubMed: 21647200]
36. Chen J, Huang XF. The signal pathways in azoxymethane-induced colon cancer and preventive implications. Cancer Biol Ther. 2009; 8:1313–7. [PubMed: 19502780]
37. De Robertis M, Massi E, Poeta ML, Carotti S, Morini S, Cecchetelli L, Signori E, Fazio VM. The AOM/DSS murine model for the study of colon carcinogenesis: From pathways to diagnosis and therapy studies. J Carcinog. 2011; 10:9. [PubMed: 21483655]
38. Adibi SA. Regulation of expression of the intestinal oligopeptide transporter (Pept-1) in health and disease. Am J Physiol Gastrointest Liver Physiol. 2003; 285:G779–88. [PubMed: 14561585]
39. Thwaites DT, Anderson CM. H+-coupled nutrient, micronutrient and drug transporters in the mammalian small intestine. Exp Physiol. 2007; 92:603–19. [PubMed: 17468205]
40. Newstead S. Towards a structural understanding of drug and peptide transport within the proton-dependent oligopeptide transporter (POT) family. Biochem Soc Trans. 2011; 39:1353–8. [PubMed: 21936814]
41. Dalmasso G, Charrier-Hisamuddin L, Nguyen HT, Yan Y, Sitaraman S, Merlin D. PepT1-mediated tripeptide KPV uptake reduces intestinal inflammation. Gastroenterology. 2008; 134:166–78. [PubMed: 18061177]
42. Luger TA, Scholzen TE, Brzoska T, Bohm M. New insights into the functions of alpha-MSH and related peptides in the immune system. Ann N Y Acad Sci. 2003; 994:133–40. [PubMed: 12851308]
43. Brzoska T, Luger TA, Maaser C, Abels C, Bohm M. Alpha-melanocyte-stimulating hormone and related tripeptides: biochemistry, antiinflammatory and protective effects in vitro and in vivo, and future perspectives for the treatment of immune-mediated inflammatory diseases. Endocr Rev. 2008; 29:581–602. [PubMed: 18612139]

44. Laroui H, Dalmasso G, Nguyen HT, Yan Y, Sitaraman SV, Merlin D. Drug-loaded nanoparticles targeted to the colon with polysaccharide hydrogel reduce colitis in a mouse model. Gastroenterology. 2010; 138:843–53. e1–2. [PubMed: 19909746]
45. Kannengiesser K, Maaser C, Heidemann J, Luegering A, Ross M, Brzoska T, Bohm M, Luger TA, Domschke W, Kucharzik T. Melanocortin-derived tripeptide KPV has anti-inflammatory potential in murine models of inflammatory bowel disease. Inflamm Bowel Dis. 2008; 14:324–31. [PubMed: 18092346]
46. Greten FR, Eckmann L, Greten TF, Park JM, Li ZW, Egan LJ, Kagnoff MF, Karin M. IKKbeta links inflammation and tumorigenesis in a mouse model of colitis-associated cancer. Cell. 2004; 118:285–96. [PubMed: 15294155]
47. Viennois E, Xiao B, Ayyadurai S, Wang L, Wang PG, Zhang Q, Chen Y, Merlin D. Micheliolide, a new sesquiterpene lactone that inhibits intestinal inflammation and colitis-associated cancer. Laboratory investigation; a journal of technical methods and pathology. 2014; 94:950–65. [PubMed: 25068660]
48. Wong NA, Pignatelli M. Beta-catenin--a linchpin in colorectal carcinogenesis? Am J Pathol. 2002; 160:389–401. [PubMed: 11839557]
49. DiDonato JA, Mercurio F, Karin M. NF-kappaB and the link between inflammation and cancer. Immunol Rev. 2012; 246:379–400. [PubMed: 22435567]
50. Lengyel E, Wang H, Gum R, Simon C, Wang Y, Boyd D. Elevated urokinase-type plasminogen activator receptor expression in a colon cancer cell line is due to a constitutively activated extracellular signal-regulated kinase-1-dependent signaling cascade. Oncogene. 1997; 14:2563–73. [PubMed: 9191056]
51. Rice PL, Goldberg RJ, Ray EC, Driggers LJ, Ahnen DJ. Inhibition of extracellular signal-regulated kinase 1/2 phosphorylation and induction of apoptosis by sulindac metabolites. Cancer research. 2001; 61:1541–7. [PubMed: 11245463]
52. Hagiya Y, Fukuhara H, Matsumoto K, Endo Y, Nakajima M, Tanaka T, Okura I, Kurabayashi A, Furihata M, Inoue K, Shuin T, Ogura S. Expression levels of PEPT1 and ABCG2 play key roles in 5-aminolevulinic acid (ALA)-induced tumor-specific protoporphyrin IX (PpIX) accumulation in bladder cancer. Photodiagnosis and photodynamic therapy. 2013; 10:288–95. [PubMed: 23993855]
53. Jasperson KW, Tuohy TM, Neklason DW, Burt RW. Hereditary and familial colon cancer. Gastroenterology. 2010; 138:2044–58. [PubMed: 20420945]
54. Li Y, Kundu P, Seow SW, de Matos CT, Aronsson L, Chin KC, Karre K, Pettersson S, Greicius G. Gut microbiota accelerate tumor growth via c-jun and STAT3 phosphorylation in APCMin/+ mice. Carcinogenesis. 2012; 33:1231–8. [PubMed: 22461519]
55. Laroui H, Yan Y, Narui Y, Ingersoll SA, Ayyadurai S, Charania MA, Zhou F, Wang B, Salaita K, Sitaraman SV, Merlin D. L-Ala-gamma-D-Glu-meso-diaminopimelic acid (DAP) interacts directly with leucine-rich region domain of nucleotide-binding oligomerization domain 1, increasing phosphorylation activity of receptor-interacting serine/threonine-protein kinase 2 and its interaction with nucleotide-binding oligomerization domain 1. The Journal of biological chemistry. 2011; 286:31003–13. [PubMed: 21757725]
56. Berg DJ, Davidson N, Kuhn R, Muller W, Menon S, Holland G, Thompson-Snipes L, Leach MW, Rennick D. Enterocolitis and colon cancer in interleukin-10-deficient mice are associated with aberrant cytokine production and CD4(+) TH1-like responses. J Clin Invest. 1996; 98:1010–20. [PubMed: 8770874]
57. Chen HQ, Yang J, Zhang M, Zhou YK, Shen TY, Chu ZX, Hang XM, Jiang YQ, Qin HL. Lactobacillus plantarum ameliorates colonic epithelial barrier dysfunction by modulating the apical junctional complex and PepT1 in IL-10 knockout mice. Am J Physiol Gastrointest Liver Physiol. 2010; 299:G1287–97. [PubMed: 20884889]
58. Adibi SA. The oligopeptide transporter (Pept-1) in human intestine: biology and function. Gastroenterology. 1997; 113:332–40. [PubMed: 9207295]
59. Nielsen CU, Brodin B. Di/tri-peptide transporters as drug delivery targets: regulation of transport under physiological and patho-physiological conditions. Current drug targets. 2003; 4:373–88. [PubMed: 12816347]

60. Abe F, Shibuya K, Uchida M, Takahashi K, Horinishi H, Matsuda A, Ishizuka M, Takeuchi T, Umezawa H. Effect of bestatin on syngeneic tumors in mice. Gann = Gan. 1984; 75:89–94. [PubMed: 6586596]

61. Hiltz ME, Lipton JM. Antiinflammatory activity of a COOH-terminal fragment of the neuropeptide alpha-MSH. FASEB J. 1989; 3:2282–4. [PubMed: 2550304]

62. Kelly JM, Moir AJ, Carlson K, Yang Y, MacNeil S, Haycock JW. Immobilized alpha-melanocyte stimulating hormone 10–13 (GKPV) inhibits tumor necrosis factor-alpha stimulated NF-kappaB activity. Peptides. 2006; 27:431–7. [PubMed: 16274845]

63. Brandsch M, Miyamoto Y, Ganapathy V, Leibach FH. Expression and protein kinase C-dependent regulation of peptide/H+ co-transport system in the Caco-2 human colon carcinoma cell line. The Biochemical journal. 1994; 299(Pt 1):253–60. [PubMed: 8166648]

64. Farraye FA, Odze RD, Eaden J, Itzkowitz SH. AGA technical review on the diagnosis and management of colorectal neoplasia in inflammatory bowel disease. Gastroenterology. 2010; 138:746–74. 774 e1–4. quiz e12–3. [PubMed: 20141809]

65. Bansal P, Sonnenberg A. Risk factors of colorectal cancer in inflammatory bowel disease. The American journal of gastroenterology. 1996; 91:44–8. [PubMed: 8561142]

Summary

PepT1 is highly expressed in colorectal tumor biopsies and exacerbates tumor development in murine models of colitis associated cancer. The small peptide KPV, transported by PepT1, decreases colon tumorigenesis suggesting that PepT1 is a potential therapeutic target for colon cancer.

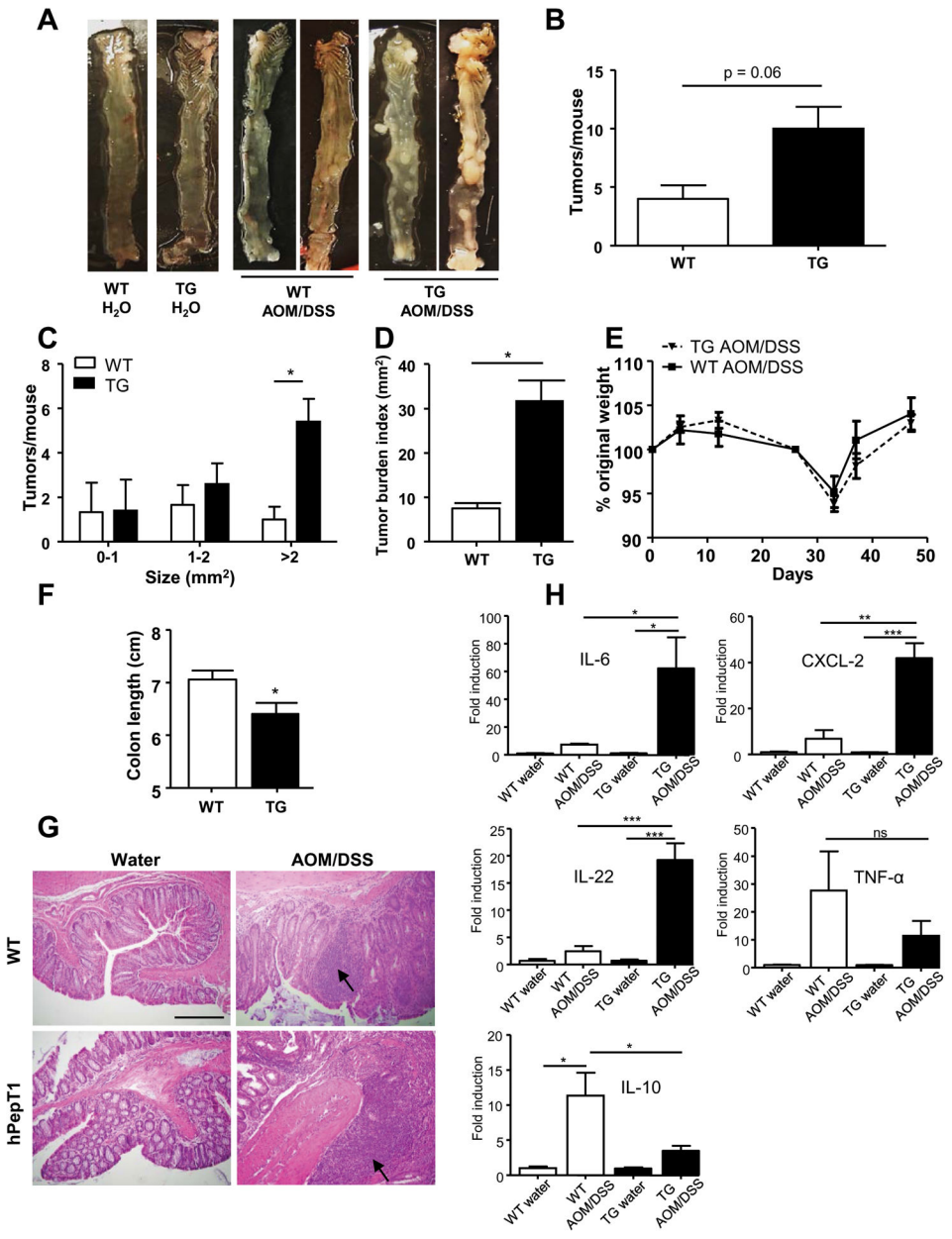

Figure 1. Inflammation and tumor growth is increased in mice that overexpress PepT1 in their intestinal epithelial cells

FVB/NJ WT and TG mice were intraperitoneally (IP) injected with AOM (10 mg/kg body weight), maintained for 7 days, and then subjected to a two-cycle DSS treatment (each cycle consisted of 7 days of 2.5% DSS and 14 days of H_2O). **A,** Representative colon samples were obtained from each experimental group at the end of the AOM/DSS protocol. **B,** Number of tumors per mouse. **C,** Tumor size was determined using a dissecting microscope fitted with an ocular micrometer. The tumor size distribution was graphed. **D,** Tumor areas for each colon were summed and were presented as the tumor burden index. **E,** AOM/DSS-treated WT and TG mice were weighed on day 0, daily during each DSS treatment, and once per week during the 2-week recovery period after each DSS treatment. The graph represents

the % values of the original day 0 weights. **F,** Colon lengths of AOM/DSS-treated WT and TG mice. **G,** Representative images of H&E-stained colonic sections from WT or TG mice that received AOM/DSS or water (control). **H**, The colonic mRNA levels of *Il-6*, *Cxcl-2*, *Il-22*, *Il-10* and *Tnf-α* were quantified by qRT-PCR and normalized to mRNA levels of the ribosomal protein, 36B4. Values are mean ± SEM (n=5 per group). Scale bar: 100 μm; arrow: inflammatory cell infiltration; * $p < 0.05$; ** $p < 0.01$; and *** $p < 0.001$.

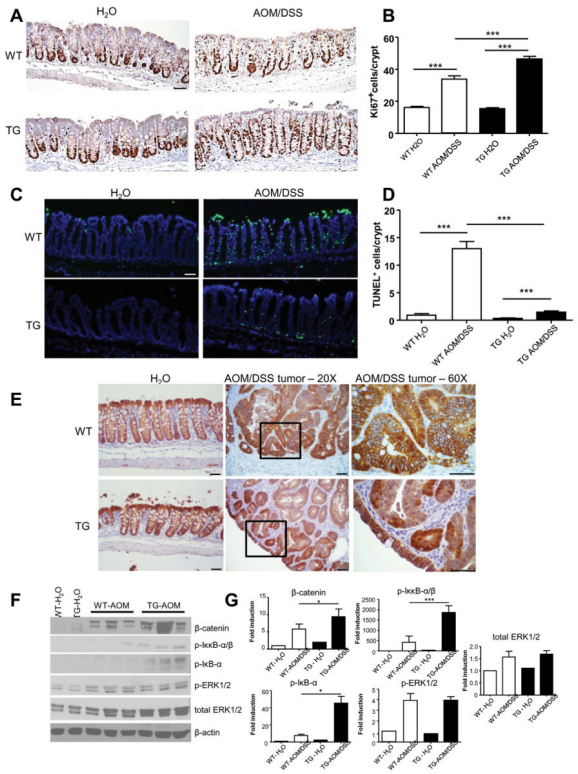

Figure 2. Overexpression of hPepT1 increases colonic epithelial proliferation, decreases epithelial apoptosis and alters tumorigenesis signaling pathways

A, The levels of epithelial cell proliferation in colonic tissue sections from WT and TG mice treated with AOM/DSS or water alone were assessed by immunohistochemistry using the proliferation marker, Ki67. **B,** $Ki67^+$ cells were counted and averaged per crypt. Values are mean ± SEM (n=5 per group). **C,** Apoptotic colonic epithelial cells were quantified using a TUNEL assay (FITC, green) and nuclei were stained with DAPI (blue). **D,** Cells positive for both TUNEL and DAPI staining were counted and averaged per crypt. Values are mean ± SEM (n=5 per group). **E,** The levels of β-catenin were assessed by immunohistochemical analysis of colonic tissue sections from WT and TG mice treated with AOM/DSS or water alone. **F,** The protein levels of phosphorylated IκκB-αβ, phosphorylated IκB-α, β-catenin, phosphorylated-ERK1/2 and total ERK1/2 in the colons of WT or TG mice treated with AOM/DSS or water alone were analyzed by Western blotting. **G,** Bar graph represents densitometric quantifications of Western blot normalized to β-actin. Scale bars: 50 μm; * $p < 0.05$; *** $p < 0.001$.

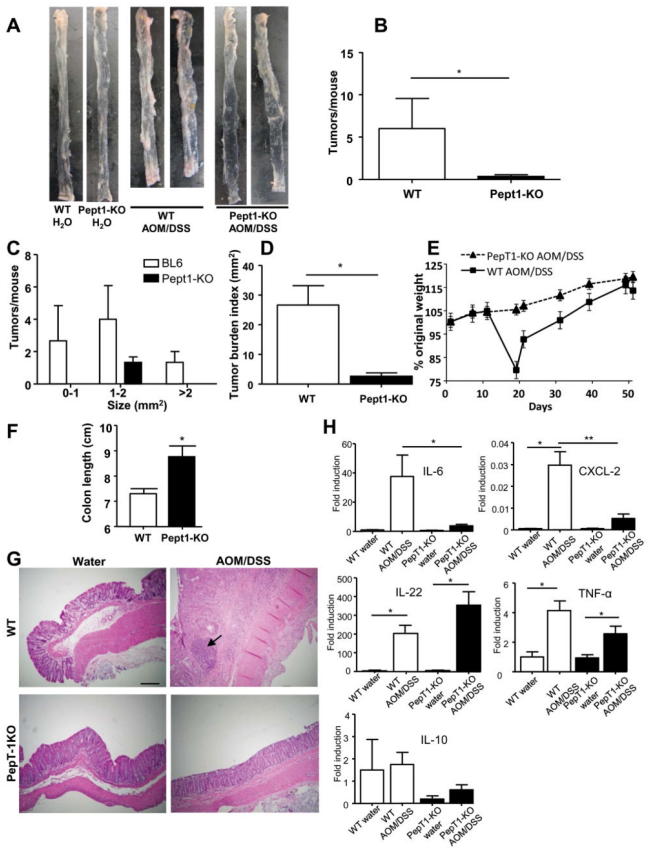

Figure 3. Inflammation and tumor growth is reduced PepT1-KO mice

WT and PepT1-KO mice were IP injected with AOM (10 mg/kg body weight) and maintained for 7 days, then subjected to two-cycle DSS treatment with each cycle consisting of 7 days of 2.5% DSS and 14 days of H_2O. **A,** Representative colons were obtained from each experimental group at the end of the AOM/DSS protocol. **B,** Number of tumors per mouse. **C,** Tumor size was determined using a dissecting microscope fitted with an ocular micrometer. The tumor size distribution was graphed. **D,** Tumor areas were summed for each colon, and were presented as the tumor burden index. **E,** AOM/DSS-treated WT and PepT1-KO mice were weighed on day 0, daily during each DSS treatment, and once per week during each 2-week post-DSS recovery period. The graph represents the % values of the original day 0 weights. **F,** Colon lengths of AOM/DSS-treated WT and PepT1-KO mice. **G,** Representative images of H&E-stained colonic sections from WT or PepT1-KO mice treated with AOM/DSS or water alone. **H**, The colonic mRNA levels of IL-6, CXCL-2, IL-22, IL-10 and TNF-α were quantified by qRT-PCR and normalized to mRNA levels of the ribosomal protein, 36B4. Values are mean ± SEM (n=4–11 per group). Scale bar: 50 μm; arrow: inflammatory cell infiltration; * $p < 0.05$; and ** $p < 0.01$.

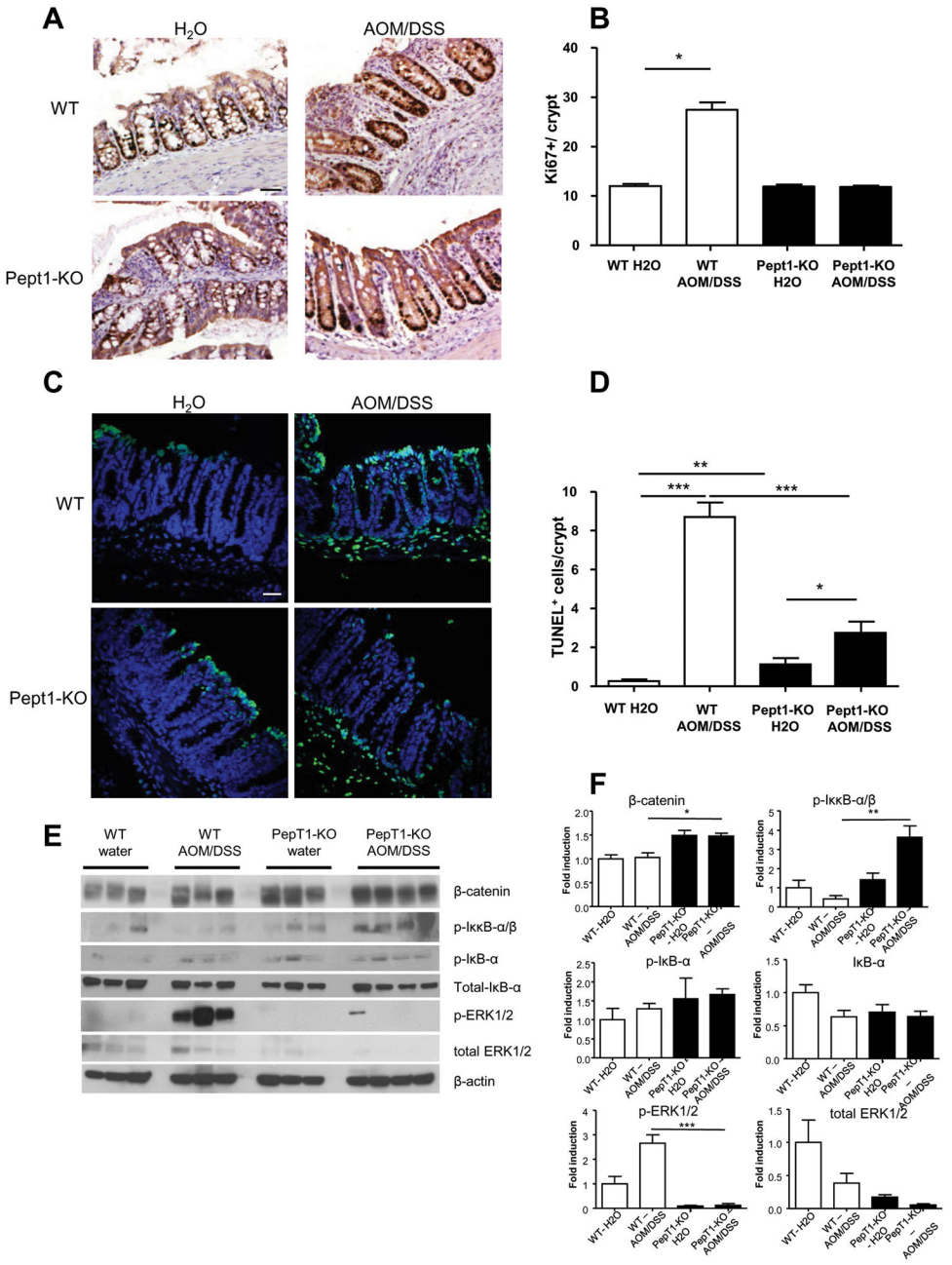

Figure 4. PepT1 knockout decreases colonic epithelial proliferation, modifies epithelial apoptosis and inhibits tumorigenesis-related signaling

A, The levels of epithelial cell proliferation in colonic tissue sections from WT and PepT1-KO mice treated with AOM/DSS or water alone were assessed by immunohistochemistry using the proliferation marker, Ki67. **B,** $Ki67^+$ cells were counted and averaged per crypt. Values are mean ± SEM (n=5–9 per group). **C,** Apoptotic colonic epithelial cells were quantified using a TUNEL assay (FITC, green), and nuclei were stained with DAPI (blue). **D,** Cells positive for both TUNEL and DAPI were counted and averaged per crypt. Values are mean ± SEM (n=5–9 per group). **E,** The protein levels of phosphorylated IκκB-αβ, phosphorylated and total IκB-α, β-catenin, phosphorylated-ERK1/2 and total ERK1/2 in the

colons of WT or PepT1-KO mice treated with AOM/DSS or water alone were analyzed by Western blotting. **F,** Bar graph represents densitometry quantifications of Western blot normalized to β-actin. Scale bars: 50 μm; * $p < 0.05$; ** $p < 0.01$; and *** $p < 0.001$.

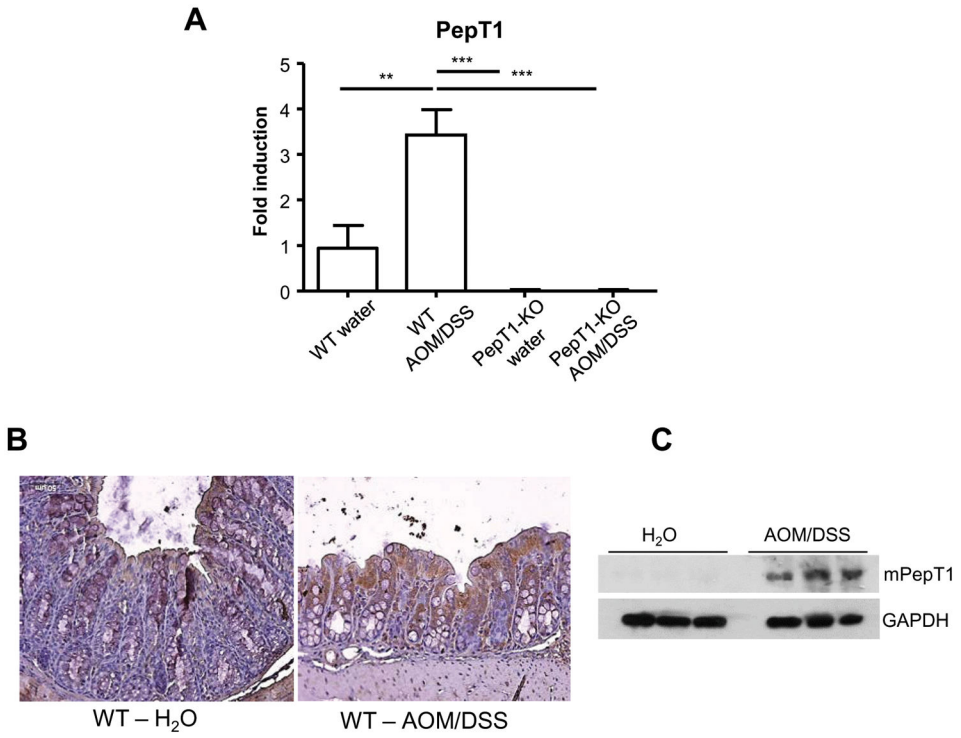

Figure 5. PepT1 expression is upregulated during colon cancer in mice

A, The colonic mRNA levels of PepT1 were quantified by qRT-PCR and normalized to mRNA levels of the ribosomal protein, 36B4. Values are mean ± SEM (n=8–9 per group). **B,** Immunohistochemical analysis of mouse PepT1 was performed on colonic tissue sections from wild-type (WT) mice treated with AOM (10 mg/kg body weight) plus two cycles of 2.5% DSS, or water alone. Microscopic images were taken at 20X magnification. **C,** Whole-colon lysates were used in Western blot analyses for mouse PepT1. β-Actin was detected as the loading control. **, $p < 0.01$ and ***, $p < 0.001$.

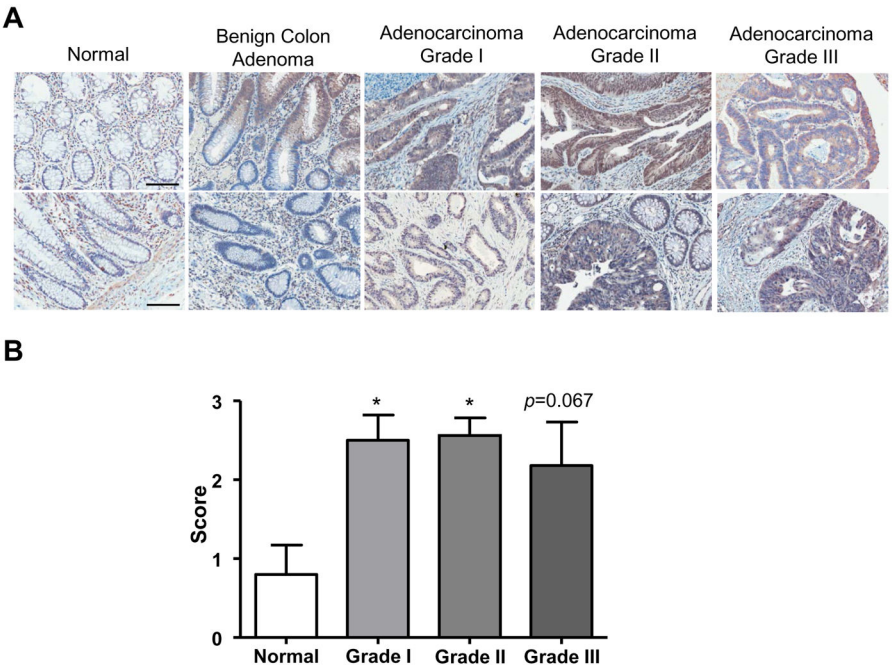

Figure 6. PepT1 expression is upregulated during colon cancer

A, Human PepT1 antibody was used to observe PepT1 levels in a human tissue microarray counterstained with hematoxylin. The tissue microarray included samples from normal patients, patients with benign colon tumors, and colon cancer patients with various stages of colon adenocarcinoma. **B,** The anti-human PepT1 stained slides were scored according two parameters (from 0 to 2): the intensity of the staining (0: absence of PepT1 positive cells, 1: low intensity staining, 2: High intensity staining) and the area of positive cells in the epithelium (0: absence of PepT1 positive cell, 1: less than the half of the epithelium is PepT1 positive, 2: the half or more of the epithelium is PepT1 positive). The intensity was indexed by the surface parameter giving one final score for each slide. Scale bars: 100 μm; *, $p < 0.05$.

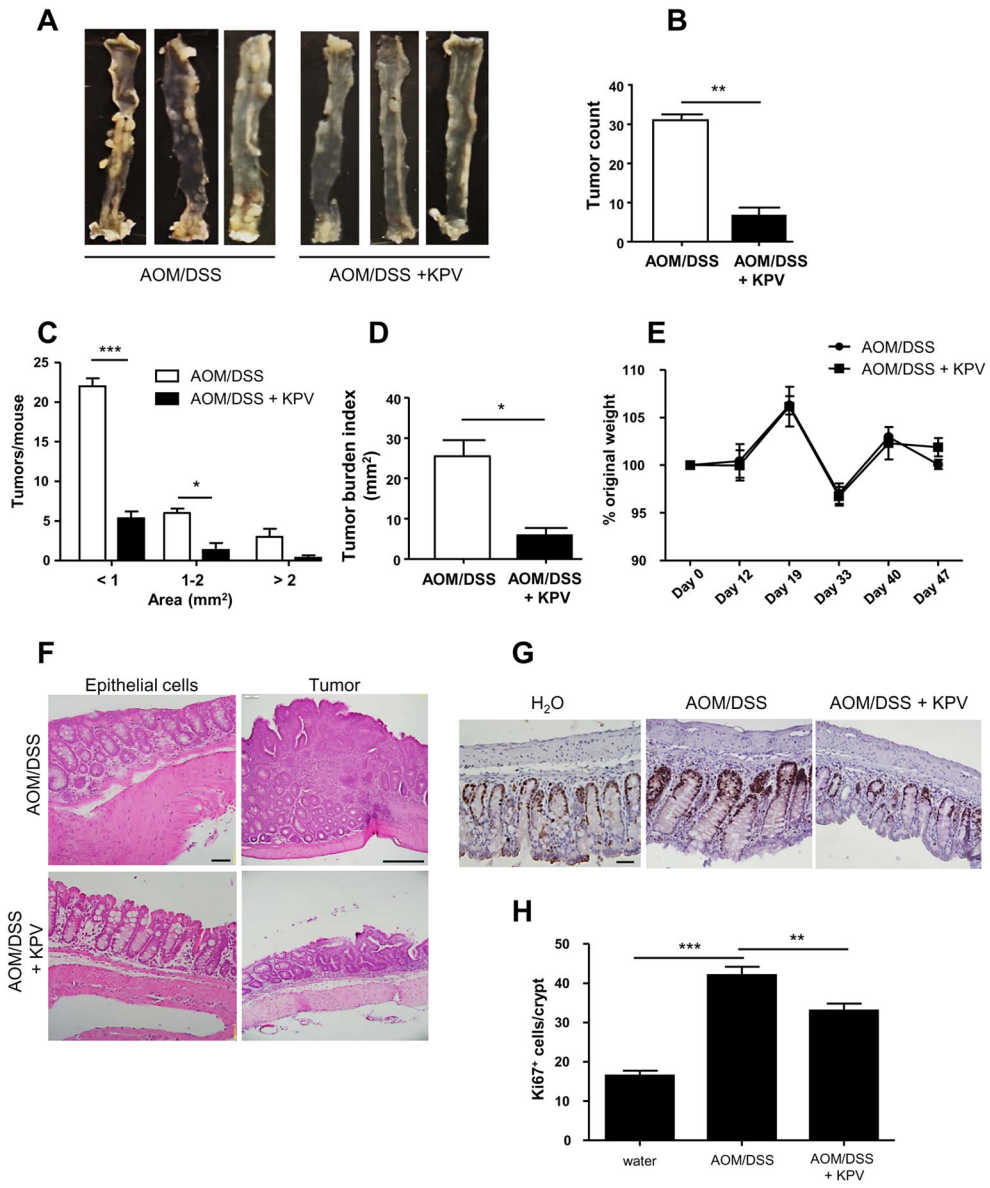

Figure 7. KPV decreases inflammation and tumorigenesis during CAC

WT mice were treated with AOM followed by two cycles of DSS, during which mice were co-treated with or without 100 μM KPV. **A,** Representative colons were obtained from each experimental group at the end of the AOM/DSS protocol. **B**, Number of tumors per mouse. **C,** Tumor size was determined using a dissecting microscope fitted with an ocular micrometer. The tumor size distribution was graphed. **D,** The tumor areas of each colon were summed, and they were presented as the tumor burden index. **E,** Mice were weighed on day 0, daily during the two DSS treatments, and once per week during the 2-week recovery period that followed each DSS or DSS/KPV treatment. The graph represents the % values of the original day 0 weight. **F,** Representative images of H&E-stained colonic sections from both experimental groups. **G,** Epithelial cell proliferation in colonic tissue sections from each experimental group was assessed by immunohistochemistry using the

proliferation marker, Ki67. **H,** $Ki67^+$ cells were counted and averaged per crypt. Values are mean ± SEM (n=6 per group). Scale bars: 50 μm; *, $p < 0.05$; **, $p < 0.01$; and ***, $p < 0.001$.

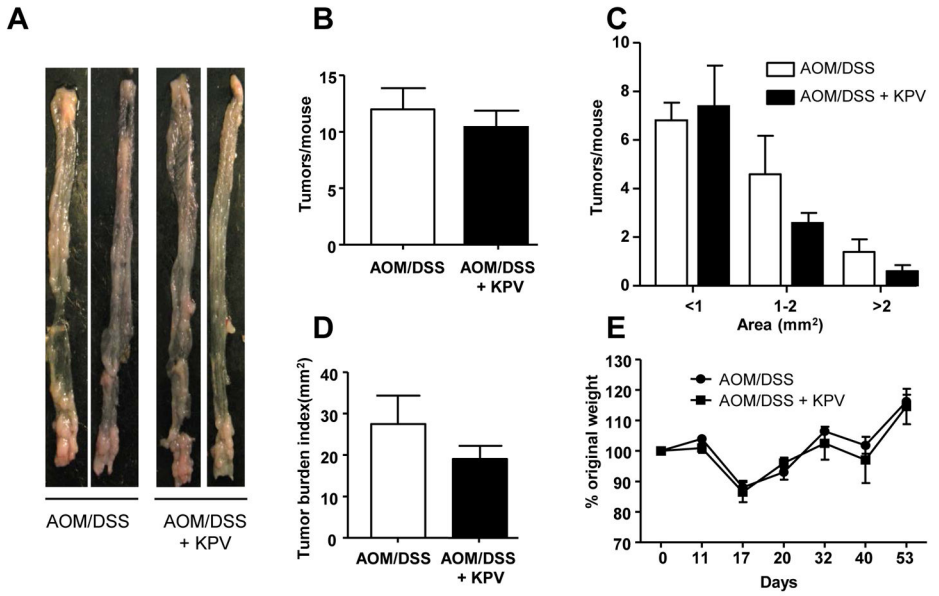

Figure 8. KPV inhibitory effect is abrogated in PepT1-KO mice

PepT1-KO mice were treated with AOM followed by two cycles of 3% DSS, during which mice were co-treated with or without 100 μM KPV. **A,** Representative colons were obtained from each experimental group at the end of the AOM/DSS protocol. **B**, Number of tumors per mouse. **C,** Tumor size was determined using a dissecting microscope fitted with an ocular micrometer. The tumor size distribution was graphed. **D,** The tumor areas of each colon were summed, and they were presented as the tumor burden index. **E,** Mice were weighed on day 0, daily during the two DSS treatments, and once per week during the 2-week recovery period that followed each DSS or DSS/KPV treatment. The graph represents the % values of the original day 0 weight. Values are mean ± SEM (n=5 per group).

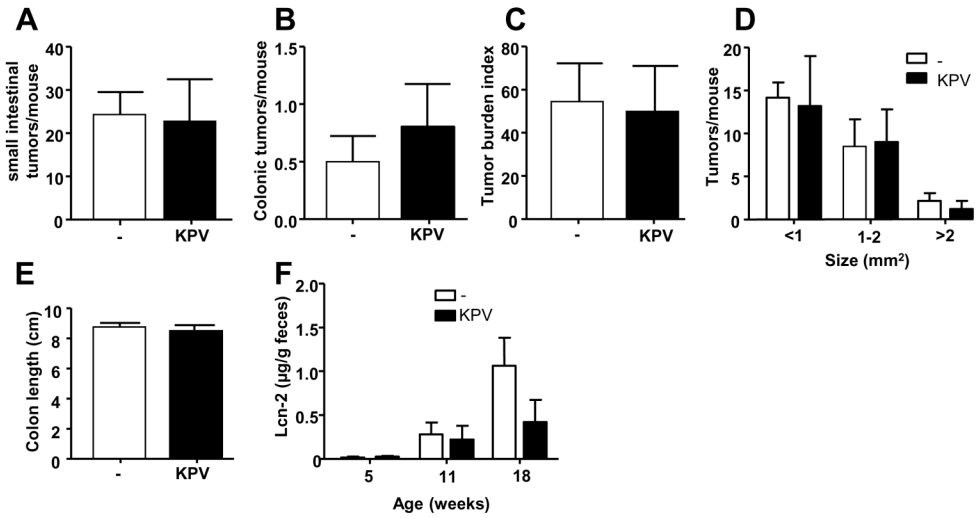

Figure 9.